Broadband Noise Limit in the Photodetection of Ultralow Jitter Optical Pulses

Wenlu Sun,[1,*] Franklyn Quinlan,[2,†] Tara M. Fortier,[2] Jean-Daniel Deschenes,[2] Yang Fu,[1] Scott A. Diddams,[2] and Joe C. Campbell[1]

[1]*Department of Electrical and Computer Engineering, University of Virginia, 351 McCormick Road, Charlottesville, Virginia 22904, USA*

[2]*National Institute of Standards and Technology, 325 Broadway, Boulder, Colorado 80305, USA*

(Received 8 August 2014; published 14 November 2014)

Applications with optical atomic clocks and precision timing often require the transfer of optical frequency references to the electrical domain with extremely high fidelity. Here we examine the impact of photocarrier scattering and distributed absorption on the photocurrent noise of high-speed photodiodes when detecting ultralow jitter optical pulses. Despite its small contribution to the total photocurrent, this excess noise can determine the phase noise and timing jitter of microwave signals generated by detecting ultrashort optical pulses. A Monte Carlo simulation of the photodetection process is used to quantitatively estimate the excess noise. Simulated phase noise on the 10 GHz harmonic of a photodetected pulse train shows good agreement with previous experimental data, leading to the conclusion that the lowest phase noise photonically generated microwave signals are limited by photocarrier scattering well above the quantum limit of the optical pulse train.

DOI: 10.1103/PhysRevLett.113.203901 PACS numbers: 42.62.Eh, 02.70.Uu, 85.60.Dw

Introduction.—Noise in photodetection can limit the fidelity by which one may determine the character of an optical field, and can corrupt electronic signals generated from optical sources. Although a property of the optical signal, shot noise is often associated with photodetection, and represents the standard quantum limit of measurements of optical phase, amplitude, and timing. Any other electronic noise source, be it thermal, amplifier, or excess photodetector noise, degrades the system performance. Therefore, operation at the shot noise limit is always preferred.

An important application that strives for quantum-limited photocurrent noise is the generation of high-spectral purity microwave signals via the detection of ultrastable optical signals. The most frequency-stable electromagnetic radiation is produced by optical sources, where lasers locked to passive reference cavities approach a frequency instability of 10^{-16} at 1 s [1], and optical clock instabilities are nearing 10^{-18} at 10^4 s [2,3]. Both the short and the long term phase stability of optical references find new utility when transferred to the microwave domain, as local oscillators for microwave atomic clocks [4], for synchronization at kilometer-scale facilities [5,6], and in radar systems [7]. The lowest noise optically derived microwave signals to date have been generated via high-speed photodetection of an ultralow jitter optical pulse train, as illustrated in Fig. 1. Here, an optical frequency comb produced by a femtosecond mode-locked laser is locked to an ultrastable optical frequency reference, transferring its fractional frequency stability to the pulse repetition rate [8]. The low jitter optical pulse train illuminates a high-speed photodetector and is transformed into an electrical pulse train. The spectrum of such a pulse train approximates a series of Dirac delta functions separated by the repetition rate. A bandpass filter centered at the desired frequency is used to select the microwave signal. In this manner, 10 GHz signals have been generated with phase noise less than −100 dBc/Hz at 1 Hz offset from the carrier [9], closely following the noise level expected from the optical reference. This is more than 40 dB below the best room-temperature microwave oscillators and comparable to the best cryogenic microwave oscillators. The corresponding 10 GHz timing jitter, obtained by extrapolating and

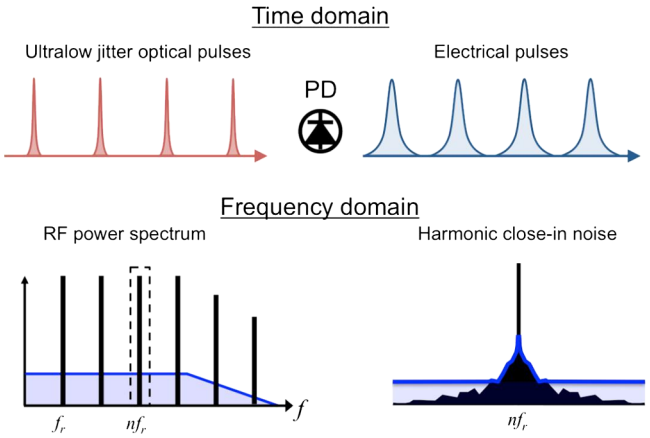

FIG. 1 (color online). Schematic diagram of photonic microwave generation via the detection of ultralow jitter optical pulses. In the lower right, the black noise sidebands represent the noise from the optical pulse train, and the blue line is the total noise after photodetection.

integrating the phase noise spectrum to the Nyquist frequency (5 GHz), is <3 fs for time scales up to 1 s.

The majority of the 10 GHz timing jitter can be attributed to the phase noise for offset frequencies 1 MHz and greater, and phase noise floors as low as −179 dBc/Hz have been demonstrated [10]. This is ~25 dB above what analysis indicates is the limit imposed by the optical pulse train, determined by the contribution of the photocurrent shot noise [11]. Additionally, circuit thermal noise and detector dark current contributions to the phase noise are sufficiently low that they also cannot explain the measured phase noise. Thus, there remains a disparity between analysis and what has been demonstrated in the phase noise far from the carrier.

To resolve the discrepancy between experiment and analysis, here we consider detection noise from sources not normally accounted for in photodiodes (PDs), namely photocarrier scattering and distributed absorption of photons within the detector. A Monte Carlo simulation has been developed that indicates that the contribution to the phase noise of this excess noise can be orders of magnitude above that of the shot noise, and can easily limit the phase stability of microwaves derived from the lowest jitter pulse trains. This constitutes an important, previously unrecognized noise source inherent in the optical to microwave conversion of ultralow jitter pulse trains.

Shot noise and photocarrier transport.—Shot noise may be described as the quantum noise arising from randomness in the photon arrival, described with Poisson statistics, that is transformed into fluctuations in the photocurrent during the photodetection process. As shown in Fig. 2, absorption of photons generates photocarriers that, when subject to an electric field, create current impulses [12]. For detectors without gain, each impulse contains the charge of a single electron, and the sum of these impulses becomes the measured photocurrent. For average photocurrents above a few milliamperes, thermal noise is smaller than shot noise, and the photocurrent noise spectral density can be represented as

$$S_i(f) = 2qI_{\mathrm{avg}}|H(f)|^2\ (\mathrm{A}^2/\mathrm{Hz}), \tag{1}$$

where q is the fundamental charge, I_{avg} is the average photocurrent, and $H(f)$ is the transfer function associated with the impulse response of the photodiode. As illustrated in Fig. 2, PDs will additionally have randomness in the impulse response, since the exact shape and width of every current impulse will depend on where in the absorptive region the photocarrier is generated, as well as on the random path taken by each photocarrier. Equation (1) can be adapted to include these effects by allowing the impulse response to vary randomly, as is often done in detectors with gain [12]. This yields

$$S_i(f) = 2qI_{\mathrm{avg}}|\langle H(f)\rangle|^2F_H, \tag{2}$$

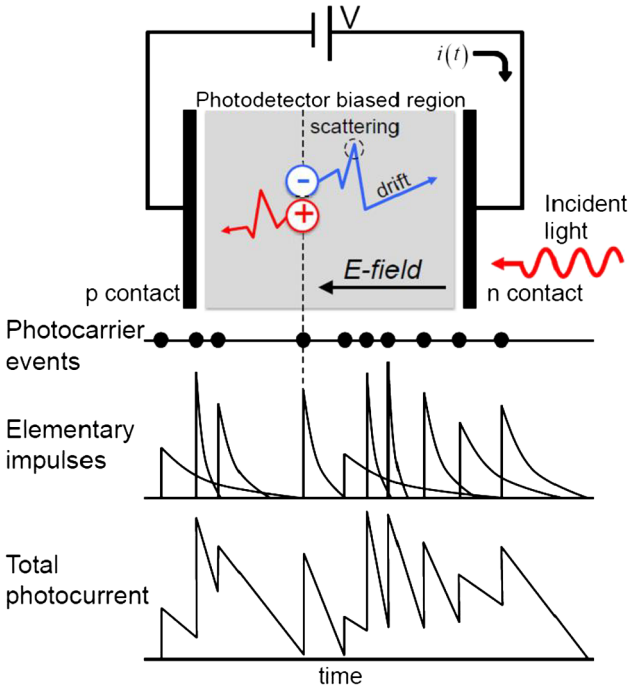

FIG. 2 (color online). Simplified schematic illustration of photocarrier transport and resulting photocurrent from a reverse-biased photodiode. Both the randomness in the timing of the photoelectron events and the shape of the elementary impulses give rise to noise in the photocurrent.

where the angled brackets indicate ensemble average, and F_H is the excess noise factor defined by

$$F_H = \langle|H(f)|^2\rangle/|\langle H(f)\rangle|^2. \tag{3}$$

By definition $F_H \geq 1$. When $F_H < 2$, the shot noise is larger than the excess noise. In the absence of gain, $F_H < 2$ is expected, justifying the exclusion of the excess noise factor and the prevalence of Eq. (1) in the description of reverse-biased PDs.

Whereas the excess noise contributes less to the total photocurrent than does the shot noise, the situation is drastically changed when considering the phase quadrature of microwaves generated by detecting ultrashort optical pulses. Here the shot noise contribution is dependent on the optical pulse width [11]. For a train of Gaussian-shaped optical pulses, the shot noise contribution to the phase noise on the nth harmonic of the repetition rate is given by

$$S_\varphi(f) = \frac{2qI_{\mathrm{avg}}|H(nf_r)|^2R}{P_\mu(nf_r)}[1-\exp\{-(2\pi nf_r\tau_G)^2\}] \times (\mathrm{rad}^2/\mathrm{Hz}), \tag{4}$$

where f_r is the pulse repetition rate, R is the system impedance, P_μ is the power in the nth harmonic, and τ_G is related to the optical pulse full width at half maximum τ_p

by $\tau_p = 2\sqrt{\ln(2)}\tau_G$. For a detector with unity quantum efficiency, this represents the quantum limit of the optical pulse timing jitter [11]. The term in square brackets in Eq. (4) is the optical pulse width–dependent improvement in the phase noise, and represents the deviation in the phase noise as compared to Eq. (1). For a 10 GHz microwave carrier generated by the detection of 1 ps duration pulses, the predicted phase noise deviation is nearly −30 dB. With the shot noise contribution to the phase noise so low, the conclusion that the excess noise can be ignored in PDs without gain needs to be revisited. Assessing the impact of the excess noise depends on calculating the random path of the photocarriers, making a quantitative analytical approach intractable. However, the problem is well suited to Monte Carlo simulation. As described below, a Monte Carlo simulation of a high-speed PD has been developed to study the impact of the excess noise, leading to good agreement with experimental results.

Model description.—The Monte Carlo tool used in this work is similar to the model in Refs. [13–16], and is based on the physical level description of carrier transport in InGaAs. The model uses a simplified nonparabolic band structure that includes the Γ, L, and X valleys in the conduction band, and heavy-hole, light-hole, and split-off valence bands. For carrier scattering, we include impurity scattering, acoustic and optical phonon scattering, and impact ionization scattering. The simulated device is a modified unitraveling carrier (MUTC) detector with an active area diameter of 50 μm, the structure of which is described in Ref. [17]. Compared to standard p-i-n detectors, the MUTC structure improves the microwave saturation power while maintaining high speed and high linearity, since only high-drift-speed electrons are employed as active carriers in the drift region. The 3 dB bandwidth is close to 20 GHz, limited by the RC time constant given by the device capacitance and the circuit's resistive load. The carrier transit time is nominally 10 ps at 18 V and 15 mA average photocurrent, but will vary according to the applied bias voltage and photocarrier density. This detector, along with a 2 GHz repetition rate optical pulse train with a center wavelength of 1 μm, was used in order to best compare with experimental results in Ref. [10].

The PD structure is divided into a one-dimensional grid. A bias voltage is established across the detector, and the electric field is calculated in each grid region using Poisson's equation. Carrier drift and scattering processes are then simulated in the structure. In each small time interval Δt the probability of photon detection is proportional to the optical intensity in that time interval. For each detected photon, the absorption depth in the photodiode is chosen randomly with probability determined by the absorption profile of the detector material. The photon-generated electrons and holes transit the undepleted and depleted regions by diffusion and drift, respectively. Carrier transport in the drift regions contributes to an impulse response. The electrical impulse responses are summed to form the total output photocurrent, i.e., the electrical pulse train. In order to achieve an average current of 15 mA with a 2 GHz pulse train, $\sim 5 \times 10^7$ electron-hole pairs are simulated for each pulse. Noise calculations are based on a train of 25 000 electrical pulses.

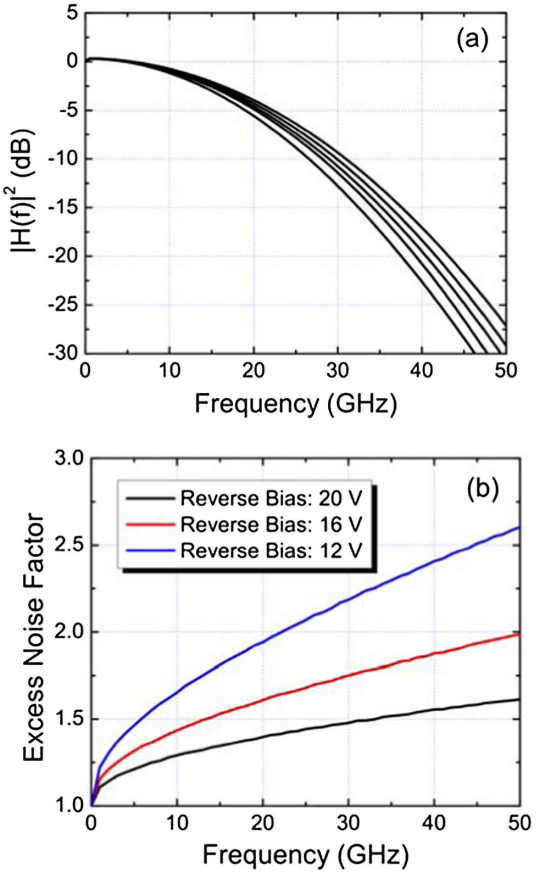

FIG. 3 (color online). (a) $|H(f)|^2$ for a few representative current impulses for 16 V bias, I_{avg} of 15 mA, and pulse width of 15 ps. (b) Calculated F_H at average current 15 mA and pulse width of 15 ps.

Representative transfer functions of simulated current impulses are shown in Fig. 3(a). All the transfer functions have the same value at zero frequency since each impulse response has the same total charge. At frequencies of 10 GHz and above, variations in the transfer function become apparent, indicating variations in the photocarrier transit time. Simulations of F_H are shown in Fig. 3(b) for different PD bias voltages and a fixed 15 mA average current and 15 ps optical pulse width. The increase of F_H with frequency is expected from the frequency dependent variation in the transfer function. For large photocurrents, the number of photocarriers is large enough that the electric field they generate is a significant fraction of the applied bias field, known as the space charge effect [18]. This causes changes in the electric field experienced by the

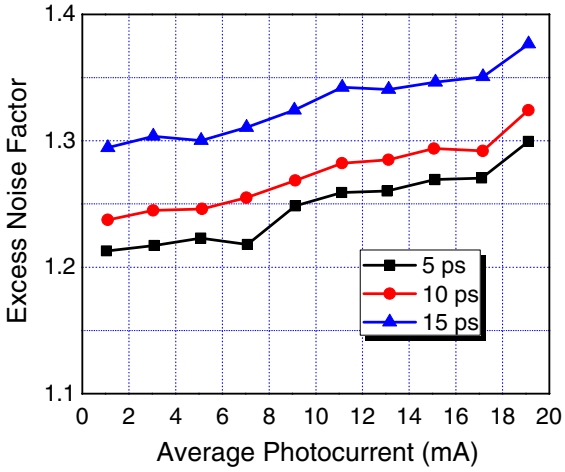

FIG. 4 (color online). Average photocurrent and optical pulse width dependence of F_H at 10 GHz.

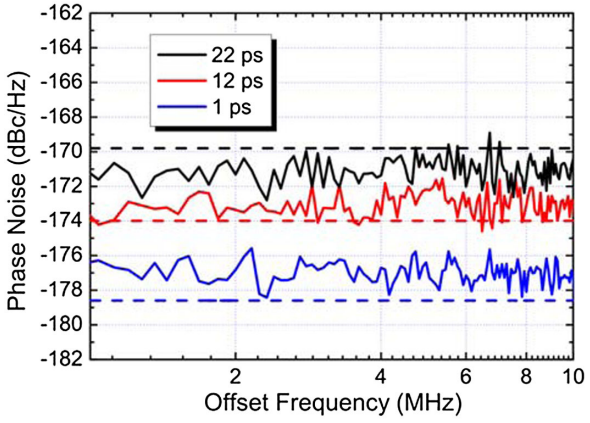

FIG. 5 (color online). Simulated single sideband phase noise level at three selected pulse widths. Dashed lines are the corresponding experimental results from Ref. [10].

photocarriers, impacting their transit time. The F_H dependence on bias voltage is due to the fact that, for lower bias voltages, space charge effects are more significant, leading to a larger variation in the photocarrier transit time. F_H is unity at zero frequency, as it must be when each impulse has the same total charge. This is the distinguishing feature between the excess noise factor of PDs with and without internal gain.

Near 10 GHz, the excess noise factor dependence on average photocurrent and optical pulse width were also explored, shown in Fig. 4. As mentioned above, the space charge effect is less significant at lower average photocurrent; therefore, the excess noise factor also tends to be lower. The optical pulse width dependence may be understood as a consequence of dynamic changes in the space charge. The narrower the optical pulse, the more likely all photocarriers experience the same space charge field, leading to a smaller variation in transit time and lower excess noise. At photocurrent levels well below 1 mA, space charge effects are negligible, and all pulse widths tend to give the same F_H.

The results in Figs. 3 and 4 show that $F_H < 2$ within the bandwidth of the detector. At 10 GHz and 18 V bias, the excess noise factor is only a 1 to 1.5 dB correction to the shot noise limit of Eq. (1), depending on the optical pulse width. At lower frequencies the correction is even smaller. However, when considering phase noise, the contribution of the excess noise can be more than an order of magnitude above the shot noise limit predicted by Eq. (4).

Phase noise simulation.—As illustrated in Fig. 2, the detector's excess noise is related to randomness in the shape of each current impulse. This results in randomness in the "center of mass" of each impulse, contributing to the timing jitter of the electrical pulse train and to the phase noise of any harmonic of f_r. This is in addition to the timing jitter due to the shot noise of Eq. (4). Since variations in the impulse shape give rise to the frequency dependence of F_H, it is this variation with frequency, not the nominal value, that indicates added phase noise. The phase noise of a photonically generated microwave was determined by multiplying the simulated pulse train with a sinusoidal reference signal whose zero crossings overlap with the arrival of the pulses, followed by a low-pass filter. Fourier transformation then yields the phase noise power spectrum. Figure 5 shows the simulated phase noise level for three selected pulse widths. Dashed lines are the corresponding experimental results from Ref. [10]. The simulated phase noise levels are all within 1–2 dB of the experimental results.

The impact of the various noise terms was analyzed by removing them individually and recalculating the resulting phase noise. These calculations are shown in Fig. 6, where the phase noise deviation versus optical pulse width is plotted. In the absence of any excess noise from the PD, only the shot noise is present, and the Monte Carlo simulation should reproduce the analytical model of Ref. [11]. The agreement between the Monte Carlo simulation and the analytical calculation is excellent, and provides an external consistency check of the model.

For MUTC devices, the impact of distributed photon absorption is minor, as it only slightly increases the noise above the shot noise limit. The dominant noise term is photocarrier scattering, placing the phase noise more than 20 dB above the shot noise limit for 1 ps pulses. Moreover, the noise does not continue to decrease with decreasing pulse width, but reaches a floor nearly 9 dB below the long pulse phase noise. Also plotted is the experimental phase noise deviation from Ref. [10], with an updated value for 1 ps pulses. The dominance of photocarrier scattering in the simulated phase noise combined with the close agreement of the phase noise level with experimental results leads to the conclusion that randomness in carrier scattering is the limit of the lowest phase noise floors yet generated by the detection of ultrashort optical pulses.

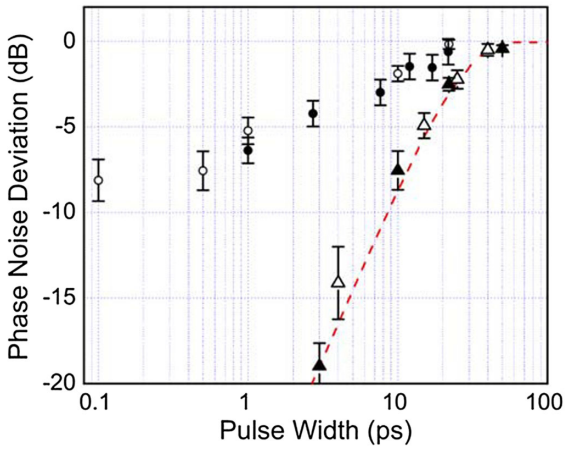

FIG. 6 (color online). Phase noise deviation from the long pulse limit. Red dash curve is the analytical calculation from Ref. [11]. Closed circle symbols are the experimental measurement from Ref. [10] with error bars. Open triangle symbols are Monte Carlo simulation of shot noise only. Closed triangle symbols are Monte Carlo simulation of shot noise and distributed absorption only. Open circle symbols are Monte Carlo simulation of shot noise, photon absorption, and carrier scattering.

Conclusion.—While contributing little to the total photocurrent noise, excess noise in reverse-biased PDs can dominate the phase noise floor of microwave signals generated by detecting ultralow jitter optical pulse trains. By developing a Monte Carlo model of carrier transport, we have evaluated the impact of photocarrier scattering and distributed absorption for high power, high linearity MUTC detectors. It was determined that scattering results in phase noise several orders of magnitude above the shot noise limit. While the impact of distributed absorption was minimal in the device studied, other detector structures, such as waveguide detectors [19], may be more sensitive to distributed absorption. Since the excess noise factor increases more slowly than the microwave power with increased photocurrent, reducing the impact of the excess noise can be achieved with higher power optical pulses. Additionally, further study of the different scattering mechanisms may lead to detector designs with lower excess noise. While this work has focused on 10 GHz generation, the transit time variance has a smaller impact at lower microwave carrier frequencies; thus, operating further from the transit time limit should lead to improved phase noise performance.

We thank W. Loh and R. Mirin for helpful comments on the manuscript. This work was supported by NIST and the DARPA PULSE program.

*ws8zp@virginia.edu
†fquinlan@boulder.nist.gov

[1] T. Kessler, C. Hagemann, C. Grebing, T. Legero, U. Sterr, F. Riehle, M. J. Martin, L. Chen, and J. Ye, Nat. Photonics **6**, 687 (2012).
[2] N. Hinkley, J. A. Sherman, N. B. Phillips, M. Schioppo, N. D. Lemke, K. Beloy, M. Pizzocaro, C. W. Oates, and A. D. Ludlow, Science **341**, 1215 (2013).
[3] B. J. Bloom, T. L. Nicholson, J. R. Williams, S. L. Campbell, M. Bishof, X. Zhang, W. Zhang, S. L. Bromley, and J. Ye, Nature (London) **506**, 71 (2014).
[4] G. Santarelli, C. Audoin, A. Makdissi, P. Laurent, G. J. Dick, and A. Clairon, IEEE Trans. Ultrason. Ferroelectr. Freq. Control **45**, 887 (1998).
[5] J. Kim, J. A. Cox, J. Chen, and F. X. Kartner, Nat. Photonics **2**, 733 (2008).
[6] J. F. Cliche and B. Shillue, IEEE Control Syst. Mag. **26**, 19 (2006).
[7] P. Ghelfi, F. Laghezza, F. Scotti, G. Serafino, A. Capria, S. Pinna, D. Onori, C. Porzi, M. Scaffardi, A. Malacarne, V. Vercesi, E. Lazzeri, F. Berizzi, and A. Bogoni, Nature (London) **507**, 341 (2014).
[8] S. A. Diddams, A. Bartels, T. M. Ramond, C. W. Oates, S. Bize, E. A. Curtis, J. C. Bergquist, and L. Hollberg, IEEE J. Sel. Top. Quantum Electron. **9**, 1072 (2003).
[9] T. M. Fortier, M. S. Kirchner, F. Quinlan, J. Taylor, J. C. Bergquist, T. Rosenband, N. Lemke, A. Ludlow, Y. Jiang, C. W. Oates, and S. A. Diddams, Nat. Photonics **5**, 425 (2011).
[10] F. Quinlan, T. M. Fortier, H. Jiang, A. Hati, C. Nelson, Y. Fu, J. C. Campbell, and S. A. Diddams, Nat. Photonics **7**, 290 (2013).
[11] F. Quinlan, T. M. Fortier, H. F. Jiang, and S. A. Diddams, J. Opt. Soc. Am. B **30**, 1775 (2013).
[12] B. E. A. Saleh and M. C. Teich, *Fundamentals of Photonics*, Wiley Series in Pure and Applied Optics (Wiley, New York, 1991), Chap. 17.
[13] W. L. Sun, X. G. Zheng, Z. W. Lu, and J. C. Campbell, IEEE J. Quantum Electron. **47**, 1531 (2011).
[14] W. L. Sun, X. G. Zheng, Z. W. Lu, and J. C. Campbell, IEEE J. Quantum Electron. **48**, 528 (2012).
[15] W. L. Sun, Y. Fu, Z. W. Lu, and J. Campbell, J. Appl. Phys. **113**, 044509 (2013).
[16] W. Sun, Z. Lu, X. Zheng, J. C. Campbell, S. J. Maddox, H. P. Nair, and S. R. Bank, IEEE J. Quantum Electron. **49**, 154 (2013).
[17] Z. Li, H. P. Pan, H. Chen, A. Beling, and J. C. Campbell, IEEE J. Quantum Electron. **46**, 626 (2010).
[18] K. J. Williams and R. D. Esman, J. Lightwave Technol. **14**, 84 (1996).
[19] S. M. Madison, J. Klamkin, D. C. Oakley, A. Napoleone, J. J. Plant, and P. W. Juodawlkis, IEEE Photonics J **3**, 676 (2011).